International Journal of Mechanical, Industrial and Aerospace Sciences
ISSN: 2517-9950
Vol:6, No:1, 2012

Numerical Simulation of the Flow Field around a Vertical Flat Plate of Infinite Extent

Marco Raciti Castelli, Paolo Cioppa and Ernesto Benini

***Abstract*—**This paper presents a CFD analysis of the flow field around a thin flat plate of infinite span inclined at 90° to a fluid stream of infinite extent. Numerical predictions have been compared to experimental measurements, in order to assess the potential of the finite volume code of determining the aerodynamic forces acting on a bluff body invested by a fluid stream of infinite extent.

Several turbulence models and spatial node distributions have been tested. Flow field characteristics in the neighborhood of the flat plate have been investigated, allowing the development of a preliminary procedure to be used as guidance in selecting the appropriate grid configuration and the corresponding turbulence model for the prediction of the flow field over a two-dimensional vertical flat plate.

***Keywords*—**CFD, vertical flat plate, aerodynamic force

I. Introduction and Background

FLOW of a fluid past bluff bodies and particularly of two-dimensional bluff bodies have been extensively studied because of their relevance to drag on vehicles and flow over ship hulls and submarines. Such flows provide rich and interesting flow dynamics of considerable engineering relevance. Bluff bodies such as plates, discs, circular and rectangular cylinders and V-shaped prisms are used in combustors to enhance scalar mixing and provide a flame-stabilizing region [1]. Investigations on some classical configurations have been done both experimentally and numerically in order to try to understand the fundamental aspects of wakes and flow-induced vibration. The most significant parameter to characterize this kind of flow separation is the Reynolds number.

The flow past a flat plate with different inclination angles (α) is characterized by fixed separation points at the edges of the plate, while in some regions the flow status is very sensitive to the Reynolds number and angle of attack.

Incoming flow normal to the plate is the most studied. Unlike flow past a normal plate, the case with a tilting plate has a different vortex shedding mechanism from the leading edge compared to the more complex shedding from the trailing edge. If attention is focused on the tilting angle, it is surprising to see that almost all the inclined plate flow cases are either studied by experiments or by potential flow theory [2] [3].

The earliest work concerned with vortex shedding from a sharp-edged plate was that of [4], dealing with the plate at 18 different angles of incidence. It is worth observing that this geometry was not truly rectangular.

Jackson (1987) [5] simulated the periodic behavior in two-dimensional laminar flow past various shapes of bodies, including flat plates aligned over a range of angles to the direction of flow: almost all inclined plates at significant high Reynolds numbers were investigated experimentally.

[6] measured Strouhal numbers for a family of rectangular cylinders with side ratios ranging from 0.04 to 1.0 and with angles of attack from 0° to 90°.

Lam (1996) [7] investigated the flow past an inclined flat plate at α=15° using phased-averaged LDA measurements. The results showed that the train of trailing edge vortices has higher vortex strength than the train of leading edge vortices.

Flat plates with sharp leading and trailing edges were also investigated (1996) [8].

[9] [10] simulated the flow over an inclined plate at α=18° and the computational results showed clearly that the wake is strongly dominated by the trailing edge vortices. It was also reported that there is no regular shedding motion of rotating vortices directly at the leading edge. Instead, behind the leading edge, a Kelvin-Helmholtz instability is detected in the free shear layer. These shear layer vortices develop into a large recirculation region attached to the leeward side of the plate.

[11] studied the transition route from steady to chaotic state for flow past an inclined flat plate and the results revealed a transition process via the sequential occurrence of the period-doubling bifurcations and the various incommensurate bifurcations.

Until now, wind tunnel tests, involving considerable time and financial resources, have been the only way to fully characterize the flow field around a structure, in order to assess its aerodynamics: in fact, due to the complexity of this subject, all the research and design work undertaken in this field has traditionally concentrated on the use of full-scale and wind tunnel analysis. As observed by [12], this has involved the use of expensive wind tunnel and data recording facilities and has required significant time and effort to obtain the desired results. However, during the 1970's 1980's there was a great deal of interest among the engineering community into a relatively new technique known as Computational Fluid

Marco Raciti Castelli is Research Associate at the Department of Mechanical Engineering of the University of Padua, Via Venezia 1, 35131 Padova, Italy (e-mail: marco.raciticastelli@unipd.it).

Paolo Cioppa is M.Sc. Student in Aerospace Engineering at the Department of Mechanical Engineering of the University of Padua, Via Venezia 1, 35131 Padova, Italy.

Ernesto Benini is Associate Professor at the Department of Mechanical Engineering of the University of Padua, Via Venezia 1, 35131 Padova, Italy (e-mail: ernesto.benini@unipd.it).

Dynamics (CFD). The advances made in high speed digital computer technology had enabled the solution of flow problems, which were described mathematically by a set of coupled nonlinear partial differential equations and the appropriate boundary conditions, in a relatively short space of time and for a low financial cost. Initially the wind engineering community largely ignored this technique due to the need for powerful computers and the errors in early modeling techniques. Nonetheless, the rapidly falling costs of computer hardware and further advances in technology in the late 1980's and early 1990's enabled CFD to be applied to the complex field of wind engineering.

CFD can nowadays be considered as a powerful design tool, whose integration into industrial development and production life-cycles is continuously rising. As observed by [9], this was made possible because of two main factors:

- the increase in computer performance and network facilities;
- the progress made in general purpose CFD software between modeling complexity and practicability within the industrial environment.

Performing CFD calculations provide knowledge about the flow in all its details, such as velocities, pressure, temperature, etc. Further, all types of useful graphical presentations, such as flow lines, contour lines and iso-lines are readily available. This stage can be compared to having completed a wind-tunnel study or an elaborate full-scale measurement campaign [14].

The present investigation was undertaken to numerically provide information on flow past a vertical flat plate and also to assess the CFD prediction potential by the comparison of the predicted results with the findings of Fage and Johansen [4] for a flat plate at an angle α = 90 °.

II. The Case Study

Fage and Johansen experiments [4] were made on a flat, sharp-edged rectangular steel plate, whose main dimensions are reported in Table I.

TABLE I
MAIN GEOMETRICAL FEATURES OF THE VERTICAL FLAT PLATE ADOPTED BY FAGE AND JOHANSEN [4]

Denomination	Value [m]
l	2.1336
b	0.15113
s	0.00453

The cross-section of the plate, normal to the span, is shown in Fig.1. To obtain the necessary rigidity, one surface (the front) was flat, and the other was slightly tapered from the centre, where the thickness is 3% of the chord, towards the sharp edges.

The forces on the plate, inclined at various angles to the wind were estimated, for two-dimensional flow, from observations of pressure taken around the median section. The pressure distribution over the front surface was measured at a wind speed of 15.25 m/s.

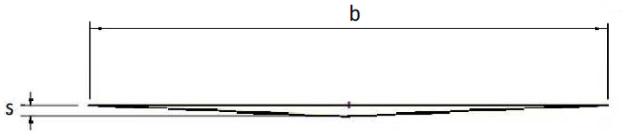

Fig. 1 Cross section of the flat plate, normal to the span

The values of the normal force coefficient k_N, were estimated from the pressure coefficients along the plate, in formulas:

$$(p - p_0)/\rho V^2 \quad (1)$$

The estimated values of k_N are given in Table II (2nd column) for all the measured angles of attack. The drag and lift coefficients can be obtained directly from the normal force coefficient by resolving respectively along the undisturbed wind direction and its normal direction. In this case, being α=90°, the drag and the normal coefficients are equal so like the forces, in formulas:

$$F_N = k_N(b\rho V_0^2) = 45.85 \text{ N} \quad (2)$$

$$C_D = F_x/(\tfrac{1}{2}\rho b V_0^2) = 0.198 \quad (3)$$

TABLE II
ESTIMATED VALUES OF K_N FOR DIFFERENT PLATE INCLINATION ANGLES (FROM: [4]). THE RED RECTANGLE EVIDENCES THE NUMERICAL DATA ADOPTED AS A REFERENCE FOR PRESENT COMPUTATIONS

α°	k_N. Wind tunnel. (A)	k_N. Kirchhoff-Rayleigh. (B)	k_N. Ratio of wind-tunnel k_N to theoretical k_N. (C)	Wind-tunnel values of $(p_m - p_0/\rho V_0^2)$ (D)	$(V_1/V_0)^2$. (E)
0	0	0	—	—	—
3	0·165	0·040	4·10	—	—
6	0·345	0·075	4·60	—	—
9	0·445	0·110	4·05	—	—
15	0·425	0·170	2·50	—	—
20	0·470	0·215	2·20	—	—
30	0·645	0·280	2·30	−0·462	1·92
40	0·785	0·335	2·35	−0·544	2·09
50	0·900	0·375	2·40	−0·615	2·23
60	0·985	0·405	2·45	−0·664	2·33
70	1·035	0·425	2·45	−0·680	2·36
80	1·060	0·435	2·45	−0·688	2·38
90	1·065	0·440	2·45	−0·690	2·38

III. Spatial Domain Discretization

All the meshes which were adopted in the present work had common geometric features, except for the areas close to the flat plate. Inlet and outlet boundary conditions were placed respectively 12 chords upwind and 25 chords downwind with respect to the plate, allowing a full development of the wake. The discretization of the computational domain into macro-areas led to two distinct sub-grids:

- A rectangular outer zone, determining the overall calculation domain, with a circular opening centered on the flat plate;
- A circular inner zone, containing the vertical flat plate. It has no physical significance: its aim is to allow a precise dimensional control of the grid elements in the area close to

the flat plate by adopting a first size function operating from the plate to the control circle itself and a second size function operating from the control circle to the whole computational domain.

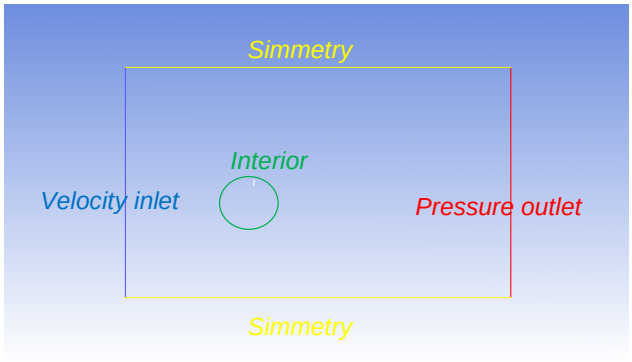

Fig. 2 Boundary conditions of the computational domain

Table III
MAIN GEOMETRICAL FEATURES THE MOD1 GRID

Mesh name	MOD1
Uniform grid spacing on the flat plate [mm]	1
Grow factor from the flat plate to the control circle [-]	1.1
Maximum grid spacing on the control circle [mm]	5
Maximum grid spacing on the computational domain [mm]	100

TABLE IV
MAIN GEOMETRICAL FEATURES THE MOD2 GRID

Mesh name	MOD2
Uniform grid spacing on the flat plate [mm]	1.5
Grow factor from the flat plate to the control circle [-]	1.1
Maximum grid spacing on the control circle [mm]	5
Maximum grid spacing on the computational domain [mm]	100

Two *symmetry* boundary condition were used for the two side walls. The circumference around the circular opening centered on the flat plate was set as an *interface*, thus ensuring the continuity of the flow field.

Fig. 2 shows the boundary conditions of the computational domain.

TABLE V
MAIN GEOMETRICAL FEATURES THE MOD3 GRID

Mesh name	MOD3
Uniform grid spacing on the flat plate [mm]	2
Grow factor from the flat plate to the control circle [-]	1.1
Maximum grid spacing on the control circle [mm]	5
Maximum grid spacing on the computational domain [mm]	100

TABLE VI
Main geometrical features the MOD4 grid

Mesh name	MOD4
Uniform grid spacing on the flat plate [mm]	4
Grow factor from the flat plate to the control circle [-]	1.1
Maximum grid spacing on the control circle [mm]	10
Maximum grid spacing on the computational domain [mm]	100

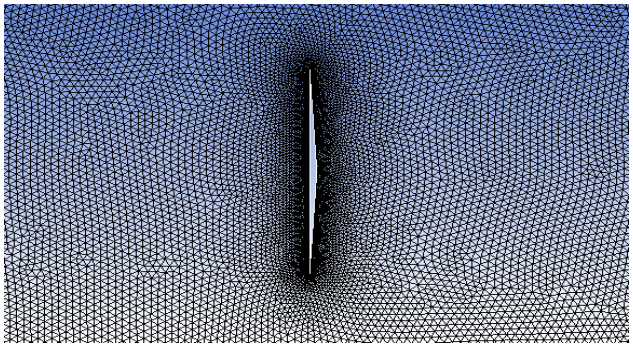

Fig. 3 Near-plate mesh, MOD1

An unstructured mesh was chosen, in order to reduce engineering time to prepare the CFD simulations and also in order to test the prediction capability of a very simple grid. Considering their features of flexibility and adaption capability, unstructured meshes are in fact very easy to obtain, also for complex geometries, and often represent the “first attempt” in order to get a quick response from the CFD in engineering work.

In order to test the numerical code sensitivity to grid resolution, four different near-plate mesh were analyzed in the present work. Tables from III to VI shows the main features of the adopted mesh configurations, which are also reproduced in Figs. 3 to 6. While Fig. 7 displays a view of the computational domain grid, showing also the control circle.

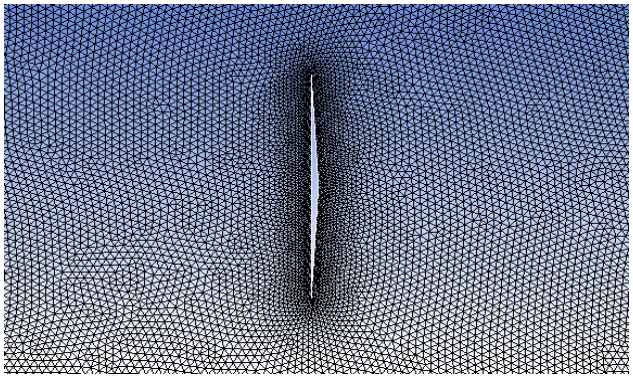

Fig. 4 Near-plate mesh, MOD2

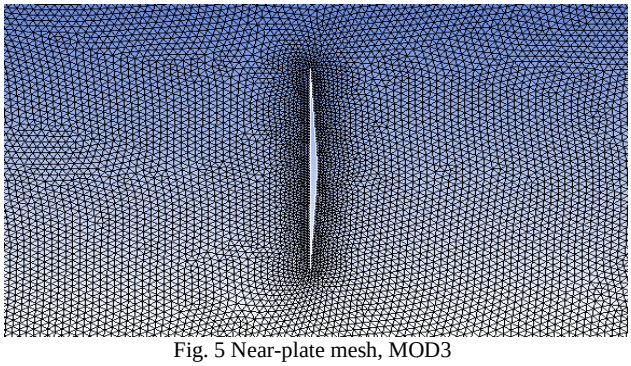

Fig. 5 Near-plate mesh, MOD3

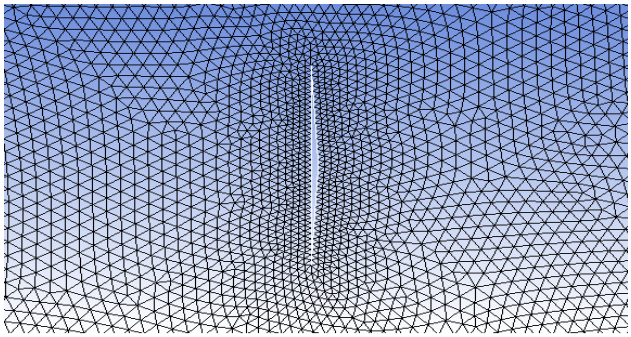

Fig. 6 Near-plate mesh, MOD4

IV. Turbulence Models and Convergence Criteria

The CFD software Ansys Fluent ® was employed to find the surface pressure distribution on the vertical flat plate. The surface pressure distribution was integrated along the upwind and downwind faces of the flat plate, in order to obtain a net force vector acting on the horizontal direction.

Calculations were completed using the following turbulence models:

- Standard k- ε;
- Realizable k- ε with Standard Wall Functions (SWF);
- Realizable k-ε with Non-Equilibrium Wall Functions (NEWF);
- NRG k-ε.

Calculations were performed until small residual values were obtained (~10^{-5}). Each simulation, performed on a 8 processor, 2.33 GHz clock frequency computer, required a total CPU time of about 1 hour.

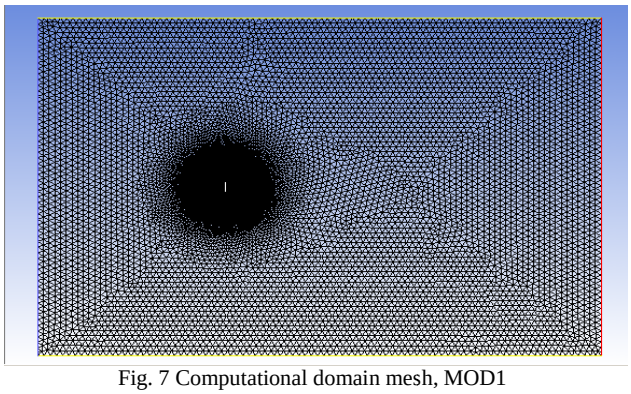

Fig. 7 Computational domain mesh, MOD1

V. Results And Discussion

Fig. 8 represents a comparison between experimental and numerical predicted drag coefficients as a function of both grid spacing and turbulence models. As can be clearly seen, the best results were registered for k-epsilon standard turbulence model and MOD3 grid spacing. The resulting drag coefficient deviation can be determined as:

$$[(C_{D,numerical} - C_{D,experimental})/C_{D,experimental}]\cdot 100 = -7.4\ \% \qquad (4)$$

It can also be observed that the influence of grid spacing on the numerical results is completely negligible, as already discussed by Raciti Castelli et al. [15] for a flow interacting normally to a square model.

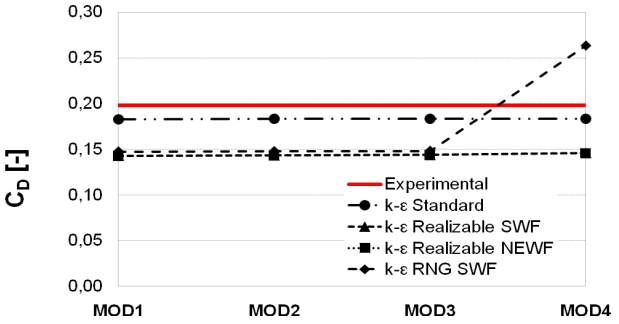

Fig. 8 Comparison between experimental and numerical drag coefficients, the marked deviation observed for MOD4 Realizable k-ε with SWF is due to non-convergence of the numerical solution

The analysis of the flow field across the vertical flat plate proceeded by means of the exploration of the velocity profiles across the boundaries of the dead-air region, along a line normal to the edge and the undisturbed wind direction at several distances (reported in Table VII) behind the plate, as represented in Fig. 9.

TABLE VII
Distance Of The Vertical Measurement Lines From The Flat Plate Edge

Denomination	x_i [m]	y/b [-]
Case 1	0.0049	0.50 – 0.66
Case 2	0.0127	0.50 – 0.70
Case 3	0.0254	0.50 – 0.73

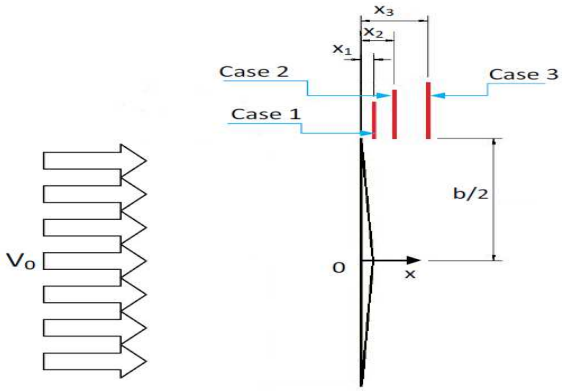

Fig. 9 Vertical measurement lines close to the flat plate

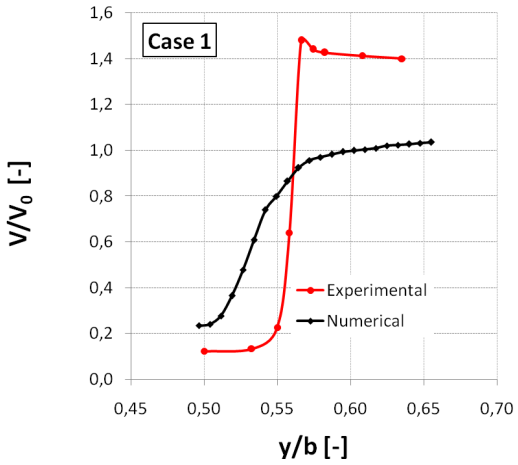

Fig. 10 Comparison between experimentally measured normalized velocities across the flat plate boundary (from: [4]) and numerical predictions, Case 1

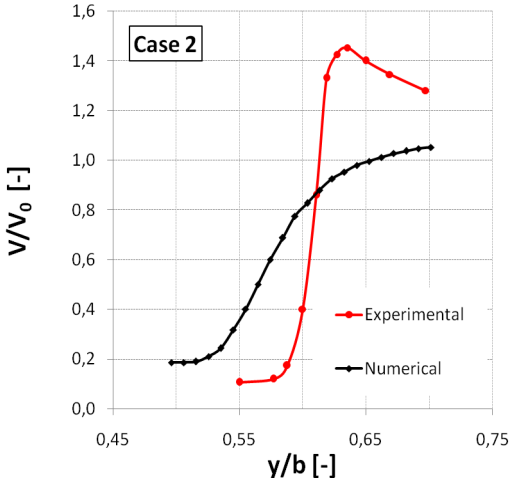

Fig. 11 Comparison between experimentally measured normalized velocities across the flat plate boundary (from: [4]) and numerical predictions, Case 2

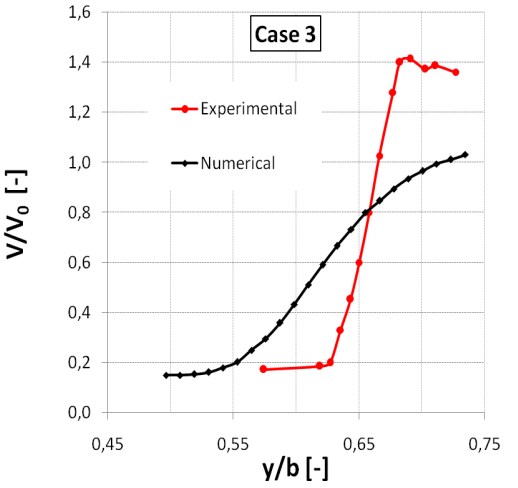

Fig. 12 Comparison between experimentally measured normalized velocities across the flat plate boundary (from: [4]) and numerical predictions, Case 3

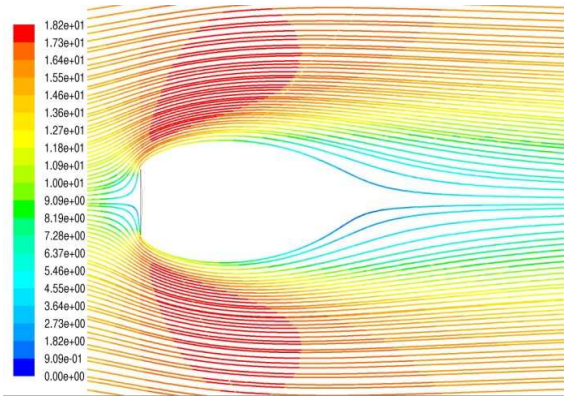

Fig. 13 Absolute pathlines across the vertical flat plate

The comparison between experimental measurements and numerical predictions is shown in Figs. 10, 11 and 12. These curves show very clearly the rapid increase of velocity across the dead-air boundary at each edge of the plate. It can also be noticed that the numerical code is not fully able to reproduce the sudden increase in flow velocity: on the contrary, a smooth velocity increase is registered, as can be noticed by Fig. 13, showing the numerically determined absolute path lines across the vertical flat plate. Further work should be done, in order to investigate the capability of LES-DES based numerical simulations to correctly reproduce the sudden velocity increase across the dead-air boundary region.

VI. Conclusions And Future Work

In this paper a CFD analysis of the flow field around a thin flat plate of infinite span, inclined at 90° to a fluid stream of infinite extent, was presented.

Numerical predictions were compared to experimental measurements, in order to assess the potential of the finite volume code of determining the aerodynamic forces acting on a bluff body invested by a fluid stream.

Several turbulence models and spatial node distributions were tested. Standard k-ε turbulence model proved to be the best option as far as the prediction of the aerodynamic drag is concern, while it was observed that the influence of grid spacing on the numerical results is completely negligible. The numerical code prediction capabilities proved to be quite good, being the experimental drag coefficient underestimated of the 7.4% on the contrary, and the numerical code capabilities to predict the rapid increase of velocity across the dead-air boundary at each edge of the plate resulted quite poor, being numerical velocity increases much smoother than the experimental ones. Further work is required in order to investigate the capability of LES-DES based numerical simulations.

Acknowledgements

The present work was funded by the EU FP7 Hoverspill project, Multi Environment Air Cushion Oil Spill Fast Response & Post Emergency Remediation System, Grant No. 234209.

NOMENCLATURE

b [m]	plate chord
C_D [-]	drag coefficient
F_N [N]	normal force
l [m]	plate length in the span-wise direction
k_N [-]	normal force coefficient = (normal force per unit length)/$\rho b V_0^2$
p [Pa]	pressure at any point of the field
p_0 [Pa]	pressure in the undisturbed air
s [m]	plate thickness
V [m/s]	average velocity at any point in the field
V_0 [m/s]	velocity of the undisturbed air relative to the plate
x_i [m]	distance of the measurement lines from the plate edge (i=1,2,3)
y [m]	vertical distance from plate edge
y/b [-]	normalized vertical distance from plate edge
α [°]	plate angle of incidence
μ [Pa·s]	air dynamic viscosity
ρ [kg/m^3]	unperturbed air density (assumed 1.225)

REFERENCES

[1] Breuer, M. and Jovicic, N., Separated flow around a flat plate at high incidence: an LES investigation. *J. Turbulence* **2** , pp. 1-15 (2001).
[2] Kiya, M. and Arie, M. An inviscid numerical simulation of vortex shedding from an inclined flat plate in shear flow. *J. Fluid Mech*. 82 , pp. 241-253 (1977).
[3] Kiya, M. and Arie, M. A contribution to an inviscid vortex-shedding model for an inclined flat plate in uniform flow. J. Fluid Mech. 82 , pp. 223-240 (1977) .
[4] Fage, A. and Johansen, F.C. On the flow of air behind an inclined flat plate of infinite span. *Brit. Aero. Res. Coun. Rep. Memo*. 1104 , pp. 81-106 (1927).
[5] Jackson, C.P., A finite-element study of the onset of vortex shedding in flow past variously shaped bodies. *J. Fluid Mech*. 182 , pp. 23-45 (1987).
[6] Knisely, C.W., Strouhal numbers of rectangular cylinders at incidence: a review and new data. *J. Fluid Structures* 4 , pp. 371-393 (1990).
[7] Lam, K.M., Phase-locked eduction of vortex shedding in flow past an inclined flat plate. *Phys. Fluids* 8 , pp. 1159-1168 (1996).
[8] Chen, J.M. and Fang, Y.-C., Strouhal numbers of inclined flat plates. *J. Wind Eng. Ind. Aerodyn*. 61 , pp. 99-112 (1996).
[9] Breuer, M. and Jovicic, N., Separated flow around a flat plate at high incidence: an LES investigation. *J. Turbulence* **2** , pp. 1-15 (2001).
[10] Breuer, M., Jovicic N. and Mazaev, K., Comparison of DES, RANS and LES for the separated flow around a flat plate at high incidence. *Int. J. Num. Meth. Fluids* 41 , pp. 357-388 (2003).
[11] Zhang, J., Liu, N.-S. and Lu, X.-Y., Route to a chaotic state in fluid flow past an inclined flat plate. *Phys. Review*. E. 79 , pp. 045306: 1-4 (2009).
[12] Easom, G. J., *Improved Turbulence Models for Computational Wind Engineering*, PhD Thesis, submitted to the University of Nottingham for the degree of Doctor of Philosophy, January 2000.
[13] Caridi, D., *Industrial CFD Simulation of Aerodynamic Noise*, PhD Thesis, Università degli Studi di Napoli Federico II, 2008.
[14] Jensen, A. G., Franke, J., Hirsch, C., Schatzmann, M., Stathopoulos, T., Wisse, J., Wright, N. G., CFD Techniques – Computational Wind Engineering. In Proceedings of the International Conference on Urban Wind Engineering and Building Aerodynamics – Impact of Wind and Storm on City Life and Built Environment – Working Group 2, *COST Action C14*, Von Karman Institute, Rode-Saint-Genèse (Belgium), 2004.
[15] Raciti Castelli, M., Castelli, A., Benini, E., Modeling Strategy and Numerical Validation of the Turbulent Flow over a two-Dimensional Flat Roof, *World Academy of Science, Engineering and Technology*, 79 (2011).